Hildegard Curtius*, Gabriele Kaiser, Norman Lieck, Murat Güngör, Martina Klinkenberg, and Dirk Bosbach

# Spent $UO_2$ TRISO coated particles – instant release fraction and microstructure evolution

**Abstract:** The impact of burn-up on the instant release fraction (IRF) from spent fuel was studied using very high burn-up $UO_2$ fuel (~ 100 GWd/t) from a prototype high temperature reactor (HTR). TRISO (TRi-structural-ISO-tropic) particles from the spherical fuel elements contain $UO_2$ fuel kernels (500 µm diameter) which are coated by three tight layers ensuring the encapsulation of fission products during reactor operation. After cracking of the tight coatings $^{85}Kr$ and $^{14}C$ as $^{14}CO_2$ were detected in the gas fraction. Xe was not detected in the gas fraction, although ESEM (Environmental Scanning Electron Micoscope) investigations revealed an accumulation in the buffer. $UO_2$ fuel kernels were exposed to synthetic groundwater under oxic and anoxic/reducing conditions. U concentration in the leachate was below the detection limit, indicating an extremely low matrix dissolution. Within the leach period of 276 d $^{90}Sr$ and $^{134/137}Cs$ fractions located at grain boundaries were released and contribution to IRF up to max. 0.2% respectively 8%. Depending on the environmental conditions, different release functions were observed. Second relevant release steps occurred in air after ~ 120 d, indicating the formation of new accessible leaching sites. ESEM investigations were performed to study the impact of leaching on the microstructure. In oxic environment, numerous intragranular open pores acting as new accessible leaching sites were formed and white spherical spots containing Mo and Zr were identified. Under anoxic/reducing conditions numerous metallic precipitates (Mo, Tc and Ru) filling the intragranular pores and white spherical spots containing Mo and Zr, were detected. In conclusion, leaching in different geochemical environments influenced the speciation of radionuclides and in consequence the stability of neoformed phases, which has an impact on IRF.

***Corresponding author: Hildegard Curtius,** Institute of Energy and Climate Research (IEK-6) Nuclear Waste Management and Reactor Safety, Research Center Jülich, 52425 Jülich, Germany, e-mail: h.curtius@fz-juelich.de

**Gabriele Kaiser, Norman Lieck, Murat Güngör, Martina Klinkenberg, Dirk Bosbach:** Institute of Energy and Climate Research (IEK-6) Nuclear Waste Management and Reactor Safety, Research Center Jülich, 52425 Jülich, Germany

**Keywords:** Spent fuel, high burn-up, leaching experiments, instant release fraction, microstructure evolution.

DOI 10.1515/ract-2014-2354
Received October 20, 2014; accepted December 9, 2014

## 1 Introduction

The reference inventory of high-level nuclear wastes designated for geological disposal in Germany as used within the preliminary safety assessment for a geological repository in the Gorleben salt dome ("vorläufige Sicherheitsanalyse Gorleben", vSG) includes various types of spent nuclear fuels from research and prototype reactors, besides LWR spent fuels and vitrified high-level wastes [1]. At the IEK-6 (Research Center Jülich) investigations concentrate on $UO_2$ based fuel elements developed for the prototype VHTR reactor. Compared to $UO_2$ LWR fuel, the VHTR fuel is very different in design and in applied irradiation conditions. A fuel pebble consists of up to 10000 small $UO_2$ fuel kernels with diameters of about 500 µm, embedded in a moulded graphite sphere with a diameter of about 60 mm (Figure 1). The outer shell (5 mm thick) of such a fuel pebble represents a fuel free zone. Each TRISO coated particle (Figure 1) possesses an $UO_2$ kernel which is coated with four layers (porous carbon buffer, inner dense pyrocarbon layer (IPyC), silicon carbide (SiC) and outer dense pyrocarbon layer (oPyC)), represents a miniature fuel element of about 1 mm in diameter. Safety assessment of spent nuclear fuel disposal in a deep geological formation requires information about the release of radionuclides from the fuel after groundwater breaches the container and contacts the fuel. The fraction of the total inventory of a given radionuclide in the spent fuel available for instant release (instant release fraction, IRF) is used as source term in safety assessment models and contribute to the long-term safety analysis. Within the European project FIRST NUCLIDES the impact of burn-up on the instant radionuclide release fraction from spent $UO_2$ fuel was investigated. For $UO_2$ LWR fuel, many papers were published and experimentally determined fuel dissolution and radionuclide release rates were given for oxidizing and re-

Bereitgestellt von | Forschungszentrum Juelich
Angemeldet
Heruntergeladen am | 26.06.15 16:04

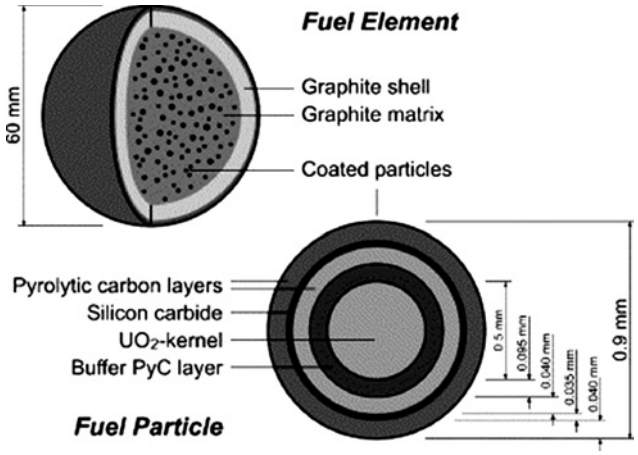


**Fig. 1:** Design of a HTR fuel element and of a TRISO coated fuel particle.

ducing conditions. A comprehensive review of the properties and performance of LWR and CANDU fuel as a waste form is given in [2–4]. Results from leaching experiments using HTR pebbles lead to the conclusion, that these fuel pebbles are well designed for direct disposal [5, 6]. The design of the moulded graphite pebble in which the coated fuel kernels are embedded represents a functional multibarrier system. As long as the coatings are intact, no large fractions of radionuclides will be released. Within this work extremely high burn-up spent $UO_2$ fuel kernels were selected as sample material. The contributions to IRF of radionuclides present in gaseous form, as water soluble salts, as metallic inclusions and the effects of leaching on the microstructure are presented.

# 2 Experimental

## 2.1 Irradiated material

At the High Flux Reactor in Petten an irradiation experiment (HFR-EU1bis) was performed to test HTR fuel pebbles for their potential for very high temperature performance and high burn-up. Five fuel pebbles from the German production line AVR GLE-4/2 were irradiated for 249 full effective power days. A comprehensive overview of the results of irradiation at increased temperature and burn up is given in [7]. Spent $UO_2$ TRISO coated particles were isolated from one of these irradiated pebbles (pebble: HFR-EU1bis/2) and used as high burn-up material within the European project FIRST NUCLIDES. In Table 1 the irradiation characteristics of the pebble HFR-EU1bis/2 are summarized. As indicated in Table 1, efpds is the acronym for effective full power days.

**Table 1:** Irradiation data for the pebble HFR1bis/2.

| | |
|---|---|
| Enrichment: | 16.76 wt % $^{235}U$ |
| Irradiation at: | High Flux Reactor Petten |
| Reactor cycles: | 10 |
| Irradiation: | 249.55 (efpds) |
| Thermal fluences: | $2.23 \times 10^{25}$ m$^{-2}$ |
| Fast fluences: | $3.98 \times 10^{25}$ m$^{-2}$ |
| Central temperature of pebbles: | 1250 °C |
| Power density: | 30 W/cm$^3$ |
| FIMA: | 10.2% (95.57 GWd/t) |

## 2.2 Radionuclide inventory

### 2.2.1 $UO_2$ TRISO coated particle

The radionuclide inventory was calculated with the OCTOPUS code at NRG (Nuclear Research and consultancy Group Petten) at the end of cool-down period of 1749 d after irradiation on 18 October 2005 and submitted to the Research Center Jülich. In order to compare these calculated values to measured values a gamma spectrometric measurement was performed. The irradiated TRISO coated particle was placed in a polyethylene tube, closed and the measurement was started. Two different detectors were attached to the gamma spectrometer; a HPGe detector type PGC 2018, Bias: 2500 V positive and a low energy germanium (LEGe) detector. The measure time was 86 400 s. The sample has a distance to the HPGe detector of 60 cm and 50 cm to the LEGe detector. For determination of the radionuclide activities the software Gamma-W version 2.44 was used. The uncertainties of the values obtained are in the range between 10 to 13%. In Table 2 the main radioisotopes and their activities (calculated and measured values) for a coated particle (CP) are summarized and discussed.

### 2.2.2 Coatings and $UO_2$ fuel kernel

In order to distinguish between the radionuclide inventory between coatings and fuel kernel a crack process was performed using a self-constructed sample device including a modified micrometer screw. With a pair of tweezers the obtained spherical fuel kernel was separated selectively from the coatings (mass: $1.97 \times 10^{-3}$ g). The coatings were placed in a 20 mL polyethylene vial. Then 10 mL Thorex reagent (mixture of 13 M nitric acid, 0.05 M hydrofluoric acid and 0.1 M aluminium nitrate) was added and leaching was performed for 7 d. The isolated fuel kernel

Bereitgestellt von | Forschungszentrum Juelich
Angemeldet
Heruntergeladen am | 26.06.15 16:04

**Table 2:** Radionuclide activities for a coated particle (CP) (mass: $2.66 \times 10^{-3}$ g) calculated with the OCTOPUS code (date: August 2010), measured activities ** for the coatings (mass: $1.97 \times 10^{-3}$ g) and for the fuel kernel (total mass: $6.88 \times 10^{-4}$ g; U mass: $6.05 \times 10^{-4}$ g) from the sample solutions (date: August 2012) and measured activities for the intact CP* by $\gamma$-measurement (date: August 2012). Uncertainties are given in blancets.

| Nuclide | Bq/CP | Bq/kernel** | Bq/coatings** | Bq/CP* |
|---|---|---|---|---|
| H-3 | $2.37 \times 10^4$ | $6.84(\pm0.34) \times 10^4$ | n.d. | n.d. |
| Sr-90 | $4.11 \times 10^6$ | $3.18(\pm0.16) \times 10^6$ | $0.17(\pm0.01) \times 10^6$ | |
| Y-90 | $4.11 \times 10^6$ | $3.18(\pm0.16) \times 10^6$ | $0.17(\pm0.01) \times 10^6$ | |
| Tc-99 | $9.86 \times 10^2$ | $1.31(\pm0.07) \times 10^3$ | $0.97(\pm0.05) \times 10^1$ | |
| Ru-106 | $2.34 \times 10^6$ | $1.33(\pm0.07) \times 10^5$ | $7.28(\pm0.36) \times 10^4$ | $3.10(\pm0.16) \times 10^5$ |
| Sb-125 | $3.95 \times 10^5$ | $1.52(\pm0.08) \times 10^4$ | $3.54(\pm0.18) \times 10^2$ | $8.10(\pm0.41) \times 10^4$ |
| Cs-134 | $1.51 \times 10^6$ | $2.58(\pm0.13) \times 10^4$ | $0.80(\pm0.04) \times 10^6$ | $0.84(\pm0.04) \times 10^6$ |
| Cs-137 | $6.47 \times 10^6$ | $4.00(\pm0.20) \times 10^5$ | $6.36(\pm0.31) \times 10^6$ | $6.56(\pm0.32) \times 10^6$ |
| Pr-144 | $2.06 \times 10^6$ | $0.35(\pm0.02) \times 10^6$ | $1.46(\pm0.07) \times 10^3$ | $0.37(\pm0.02) \times 10^6$ |
| Cer-144 | $2.05 \times 10^6$ | $0.36(\pm0.02) \times 10^6$ | $1.18(\pm0.06) \times 10^3$ | $0.31(\pm0.02) \times 10^6$ |
| Eu-154 | $2.23 \times 10^5$ | $1.14(\pm0.06) \times 10^5$ | $2.85(\pm0.14) \times 10^2$ | $1.20(\pm0.06) \times 10^5$ |
| Eu-155 | $1.22 \times 10^5$ | $4.67(\pm0.23) \times 10^4$ | $1.52(\pm0.08) \times 10^2$ | $0.49(\pm0.02) \times 10^5$ |
| U-234 | $1.42 \times 10^2$ | $1.82(\pm0.18) \times 10^2$ | n.d. | |
| U-235 | $2.95 \times 10^0$ | n.d. | n.d. | |
| U-236 | $2.59 \times 10^1$ | $3.33(\pm0.33) \times 10^1$ | n.d. | |
| Np-237 | $1.48 \times 10^1$ | n.d. | n.d. | |
| Pu-238 | $5.75 \times 10^4$ | $7.03(\pm0.35) \times 10^4$ | $2.45(\pm0.25) \times 10^2$ | |
| Pu-239 | $1.37 \times 10^4$ | $1.09(\pm0.05) \times 10^4$ | $1.41(\pm0.14) \times 10^1$ | |
| Pu-240 | $1.69 \times 10^4$ | $1.35(\pm0.07) \times 10^4$ | $1.55(\pm0.16) \times 10^1$ | |
| Pu-241 | $4.39 \times 10^6$ | $2.47(\pm0.12) \times 10^6$ | n.d. | |
| Am-241 | $3.91 \times 10^4$ | $3.11(\pm0.16) \times 10^4$ | $1.05(\pm0.11) \times 10^2$ | $2.15(\pm0.11) \times 10^4$ |
| Cm-244 | $1.20 \times 10^4$ | $0.90(\pm0.05) \times 10^4$ | $1.33(\pm0.13) \times 10^1$ | |

(mass: $6.88 \times 10^{-3.4}$ g) was placed in a 20 mL polyethylene vial and dissolved completely in 10 mL Thorex reagent within 24 h. Both sample solutions were used for further analytical steps. First the activity of tritium in the chemical form as HTO was determined. From each sample solution 100 µL were diluted with 9.9 mL water and a subboil process (70 °C) was performed. The condensate was collected and 1 mL was used for the $\beta$-measurement, performed with a Liquid Scintillation Counter (LSC, TRICARB 2200 A, Packard). Another $\beta$-measurement using 0.1 mL from each sample solution was performed and the activity of $^{241}$Pu was determined (detection limit: 0.1 Bq/sample). Then 1 mL from each sample solution was filled in a polyethylene vial and a $\gamma$-measurement was performed (HPGe detector type PGC 2018, Bias: 2500 V positive, counting time: 86 400 s, software: Gamma-W Version: 2.44: using $^{152}$Eu as standard solution with the same geometry, distance 15 cm). The uncertainty of the measured activities are in the range between 5% (high values) to 20% (low values). The activity of $^{90}$Sr was determined after the following selective separation steps; 1 mL of each sample solution was diluted with 0.67 mL of a 1 M $HNO_3$ solution. Then 1 mL of this solution was used to quantify the $^{90}$Sr activity. A column (6 mL in volume) was filled with a suspension of 1 g resin (Sr-Resin, Eichrom-Company) in 5 mL of a 2 M $HNO_3$ solution. The column was washed two times with 5 mL of a 2 M $HNO_3$ solution and then 5 ml of a 8 M $HNO_3$ solution was added. Afterwards the sample solution was added to the column. The sample vial was rinsed with 1 mL of a 8 M $HNO_3$ solution and this solution was added to the column as well. Then a washing step with 10 mL of a 8 M $HNO_3$solution was performed. The washing solution was collected. After the washing steps $^{90}$Sr was eluted by using 10 mL of a 0.05 M $HNO_3$ solution. Immediately 1 mL of the eluate was used for the $\beta$-measurement (detection limit: 0.1 Bq/sample solution). Then the activity of technetium was determined. First the washing solution of the Sr partition process was evaporated. The obtained residue was dissolved in a 2 M $HNO_3$ solution (about 2 mL) and then used as sample solution for the Tc stripping. A column (6 mL in volume) was filled with a suspension of 1 g Tc-Resin (TEVA-Resin, Eichrom-Company) in 5 mL of a 2 M $HNO_3$ solution. The column was washed two times with 5 mL of a 2 M $HNO_3$ solution. Then the sample solution was added. Washing steps were performed with 10 mL of a 2 M $HNO_3$ solution. After the washing process Tc was eluated with 10 mL of a 8 M $HNO_3$ solution. The eluate

Bereitgestellt von | Forschungszentrum Juelich
Angemeldet
Heruntergeladen am | 26.06.15 16:04

was evaporated and the residue was dissolved in 1 mL of a 2 M $HNO_3$ solution and the activity of Tc was determined by LSC (detection limit: 0.1 Bq/sample solution). An alpha-spectrometer (Octete, Ortec company, planar implanted passivated silicon-detector) was used to analyse the activities of the radionuclides U, Pu, Am, Np and Cm. 0.1 mL of both sample solutions were vaporized directly on metal disks and the measurement was performed for 250 000 s (detection limits are in the range between 0.1–0.2 mBq/mL sample solution).

## 2.3 Gas release

The self-constructed crack device was coupled to a self-constructed gas sampling tool. A spent $UO_2$ TRISO coated particle was cracked and the released gas fraction was collected. The released gases were analysed by gas chromatography and radio gas chromatography. A gas chromatograph (Siemens Sichromat II equipped with a thermal conductivity detector (detection limit: $6 \times 10^{-9}$ g/mL $N_2$ in $H_2$)) was used. The chromatograph consists of two separation columns (first column: molecular sieve 5A 80/100, length 3 m and second column: Porapack QS 80/100, length 1 m) and Argon as carrier gas was used. The radioisotopes were detected within the connected proportional gas flow-through counter. The sensitivity for $^3H$ and $^{14}C$ is respectively, 50 Bq and 3 Bq.

## 2.4 Leaching tests

Ten TRISO coated particles were cracked and the obtained $UO_2$ kernels were separated from the coatings. A low molar salt solution containing 19 mM NaCl and 1 mM $NaHCO_3$ (pH value of this solution was 7.4±0.1) was used for the leaching procedure at room temperature. Five kernels (mass of five kernels: $3.4391 \times 10^{-3}$ g; total U mass: $3.0238 \times 10^{-3}$ g) were separated from the coatings and leached in 20 mL of this low molar salt solution under oxic (air) conditions. Identical leaching experiments were performed under anoxic/reducing (96% of $Ar/H_2$ type 4.8 and 4% of $H_2$ type 3.0). 1.5 mL of solutions were taken at different time intervals. In order to keep the solid/solution ratios constant 1.5 mL of the prepared salt solution was added to each leaching flask.

Aliquots (1.5 mL) of the sample solution were filtered (450 nm) and the pH values were found to be in the range between 7.3 ± 0.1 to 7.5 ± 0.1. The stability of these pH values indicate a stable environment in which no dissolution process (consuming or releasing protons) occur so far. One milliliter of each filtrate was diluted with 9 mL of a 0.1 M $HNO_3$ solution resulting in a 10 mL sample solution. These sample solutions were analyzed according to the details given in Section 2.2.2.

## 2.5 Calculations

The Fraction of Inventory of an element $i$ released in the Aqueous Phase (FIAP) was calculated according to:

$$\mathrm{FIAP}_i = m_{i,\mathrm{aq}}/m_{i,\mathrm{SNF}} \quad (1)$$

where $m_{i,\mathrm{aq}}$ is the mass of the element $i$ in the aqueous phase (g) and $m_{i,\mathrm{SNF}}$ is the mass of the element in the SNF sample (g). The Instant Release Fraction of an element $i$ ($\mathrm{IRF}_i$) is the Fraction of Inventory of the element $i$ in the Aqueous Phase ($\mathrm{FIAP}_i$) reduced by FIAP of uranium. For the reported time period no uranium was detected in solution, hence the $\mathrm{FIAP}_i$ of the elements represent the $\mathrm{IRF}_i$. It has to be stated, that this is an assumption, because there is U in solution, but within the detection limit (see Section 3.3) by alpha-spectrometry the U concentration cannot be specified.

The Fractional Release Rate for an element $i$ ($\mathrm{FRR}_i$) in $d^{-1}$ is given by the equation:

$$\mathrm{FRR}_i = \Delta\mathrm{FIAP}_i/\Delta t \quad (2)$$

where $\Delta t$ is the time range in days and $\Delta\mathrm{FIAP}_i$ refers to the difference of the FIAPi values within this time range.

Generally spoken, the $\mathrm{FRR}_i$ describes the elemental FIAP evolution with time.

## 2.6 Microstructural characterization

Electron microscopically characterizations were performed using irradiated $UO_2$ kernels and a polished specimen of an irradiated $UO_2$ TRISO coated particle. For the polishing process the particle was embedded in a resin (Araldit DBF CH and Aradur HY 951) under vacuum. After 48 h the grinding and polishing process started. The wet grinding process was performed using sandpaper (SiC type, 35 μm and 22 μm). As last step a wet polishing of the sample was performed with sandpaper (SiC-type, 5 μm). The polishing step was performed till the $UO_2$ kernel reached 350 μm in diameter. Further grinding and polishing to the maximum diameter (500 μm) was not performed because the fuel kernel could get lost. Irradiated $UO_2$ fuel kernels were investigated before and after leaching. The sample preparation was performed by sticking the kernels on a sample holder and then the analytic

Bereitgestellt von | Forschungszentrum Juelich
Angemeldet
Heruntergeladen am | 26.06.15 16:04

examination started. For all investigations an environmental scanning electron microscope (ESEM, FEI Quanta 200 FEG instrument) was used (working distance: 10 mm; low vacuum: 0.6 mbar; acceleration voltage: 30 kV; spot size: 4). The instrument is equipped with three detectors. The gaseous large field Secondary Electron-detector was used to characterize the morphology (grain boundaries, porosity). The Back Scattered Electron-detector was used to obtain chemical information due to the Z-contrast (atomic number of the elements). With the Apollo X Drift detector the elemental mapping was performed (detection limit 0.1 wt. %).

# 3 Results

## 3.1 Radionuclide inventory

First, Table 2 reveals the calculated and measured values for the activities of $^{134/137}$Cs, $^{154/155}$Eu, $^{144}$Ce, $^{106}$Ru, $^{125}$Sb, $^{144}$Pr and $^{241}$Am present in a coated particle (CP). The mass of a coated particle is $2.66 \times 10^{-3}$ g. The determined activities (gamma-spectrometric measurements) agree with the calculated values (uncertainties of the measured values are given in blankets in Table 2). Then, after cracking of the tight coatings the fuel kernel was separated from the coatings. The fuel kernel (mass: $6.88 \times 10^{-4}$ g) and the coatings (mass: $1.97 \times 10^{-3}$ g) were treated with the Thorex reagent (described in Section 2.2.2) and after further analytic steps and measurements the activities were determined (uncertainties of the measured values are given in blankets in Table 2). The radioisotopes are quantitatively located within the fuel kernel, but Cs is an exception. Up to 95% of the inventory of Cs was present in the coatings. A high accumulation of Cs within the buffer was confirmed by ESEM investigations (see section 3.4). An excellent work performed by Barrachin *et al.* [8] summarized results from fission product behaviour in irradiated TRISO coated particles. A high Cs release was confirmed by electron probe microscopy analyses (EPMA) and calculations with MFRR code (module for fission product-release). The significant Cs release can be explained by the strong reduction of kernel oxygen potential. Under the irradiation conditions of the experiment HFR-EU1bis one can consider carbon oxidation leading to a strong decrease of fuel-kernel oxygen potential. Under this low oxygen potential (−650 kJ/mol) ternary Cs compounds are not stable and Cs-atom diffusion by U vacancies and subsequent release is considered. This low oxygen potential is the key point in Cs behaviour in $UO_2$TRISO particles, very different to $UO_2$ LWR fuel. In LWR irradiation conditions, uranium and plutonium fissions are described as oxidizing because oxygen liberated from fission is only partially associated with fission products and an amount of "free" oxygen is created corresponding to an increase of the oxygen/metal ratio and of the oxygen potential. Even for LWR fuel with comparable irradiation characteristics (10% FIMA, 1273 K) the oxygen potential determined was around −310 kJ/mol [9]. This clearly indicates that the main contribution of the reduction of the oxygen potential comes from carbon oxidation. As was mentioned before, ESEM investigations revealed an accumulation of the released Cs within the buffer. Within the buffer, the formation of intercalation compounds of $CsC_n$ can be assumed [10].

## 3.2 Gas release

Radionuclides insoluble in the $UO_2$ matrix and present in gaseous form contribute to the IRF. Especially the as mentioned irradiation conditions of the HTR fuel (high temperature, high fission rates) favour gas release by diffusion towards grain boundaries where it is released. More over gas resolution from gas bubbles occur [11]. This gas fraction also diffuses to grain boundaries where it is released. Due to the high temperature, the thermal diffusivity is high. Compared to LWR fuel [12] (fission gas release: around 2% for average burn-up of 48 GWd/t; around 8% for average burn-up of 75 GWd/t) the fission gas release from HTR fuel is expected to be significantly higher.

Within this study He, tritium and Xe were not detected in any gas sample. However ESEM investigations (Section 3.4) revealed an accumulation of Xe within the buffer region. We assumed that Xe is significantly released from the fuel kernel, hence from the fuel matrix and therefore Xe contributes significantly to the IRF. Further investigations will focus on verifying the Xe location within the coatings. An identical observation for the Xe accumulation within the buffer was already reported by Minato *et al.* [10]. Under the irradiation conditions, Xe remained in atomic form and diffused to grain boundaries. Calculations performed with the MFRR code [8] assume that the Xe fraction released is in the range of 70%, indicating that the fission gas release in HTR fuel is much higher than that of irradiated $UO_2$ LWR fuels. It is thought that the release mechanism for Xe and Cs are similar. As mentioned before, 95% of the inventory of Cs was detected in the coatings after irradiation. Considering carbon oxidation and consequently the formation of an extremely low oxygen potential, Cs is present in atomic form like Xe. A high diffusivity

Bereitgestellt von | Forschungszentrum Juelich
Angemeldet
Heruntergeladen am | 26.06.15 16:04

by U-vacancies toward grain boundaries and subsequent release for Cs and Xe is assumed.

In all gas samples high amounts of the fission gas $^{85}Kr$ were detected. Compared to the calculated inventory approximately 35% of $^{85}Kr$ was released instantaneously. In conclusion, Xe and Kr are significantly released from the fuel kernel and highly contribute to the IRF.

In all gas samples, $^{14}C$, present in the chemical form as $^{14}CO_2$ was identified and an activity of 15 ± 5 Bq was measured for this activation product. $^{14}C$ mainly is produced by neutron capture reactions involving nitrogen $^{14}N(n, p)$ and carbon $^{13}C(n, \gamma)$. Both are present as impurities in fuel. The formation of $CO_2$ can be explained by carbon oxidation, a reaction which is known to consume oxygen and hence contribute to the low oxygen potential as mentioned before. Like Xe or Kr also $^{14}C$ preferentially segregate from the fuel matrix and contributes to the IRF.

## 3.3 IRF after leaching

In the leachate the radioisotopes $^{234/235/236}U$ (detection limit: 0.73 Bq/mL, respectively 0.72 Bq/mL, respectively 0.58 Bq/mL), $^{237}Np$ (detection limit: 0.88 Bq/mL), $^{238/239/240}Pu$ (detection limit: 1.08 Bq/mL, respectively 0.96 Bq/mL, respectively 0.96 Bq/mL), $^{241}Am$ (detection limit: 1.05 Bq/mL), $^{244}Cm$ (detection limit: 0.09 Bq/mL), $^{90}Sr$ (detection limit: 0.1 Bq/mL) and $^{134/137}Cs$ (detection limit: 0.1 Bq/mL) were analysed.

Independent on geochemical redox states, $^{234/235/236}U$, $^{237}Np$, $^{238/239/240}Pu$, $^{241}Am$ and $^{244}Cm$ were not detected in solution in the time frame of investigation (276 d), hence these radioisotopes do not contribute significantly to the IRF. Especially, the low oxidative dissolution rate of the matrix under oxic conditions can be related to the very high burn-up. This high burn up cause an extensive doping of the fuel matrix, which makes the oxidative dissolution of the matrix difficult. Also, the low oxygen potential of this fuel (oxygen is consumed by carbon oxidation, see Section 3.1) create a low oxygen concentration in solution which delayed the oxidative dissolution of the fuel matrix.

Within the fuel matrix, $^{90}Sr$ is present as SrO and it also can be present in the perovskite phase ($Ba(Sr)ZrO_3$). However, up to now no significant amounts of perovskite phase were detected [8]. As SrO, $^{90}Sr$ is highly soluble within the $UO_2$ matrix and low release values are expected. For both environmental conditions the contributions of $^{90}Sr$ to the IRF were low (max 0.2%) and comparable to $UO_2$ LWR fuel [13]. It can be assumed that this $^{90}Sr$ release fraction indicates the $^{90}Sr$ inventory located

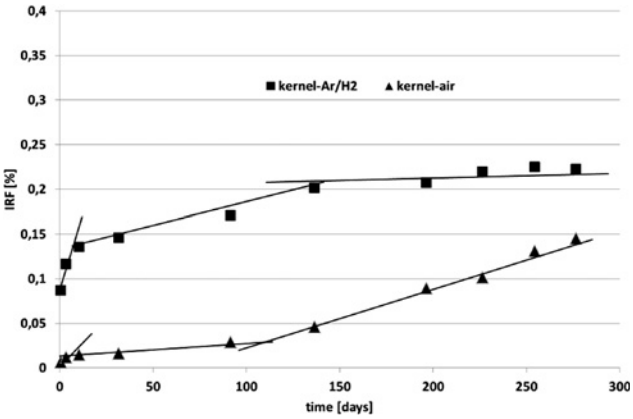


**Fig. 2:** Cumulative IRF of $^{90}Sr$ *vs.* time under oxic and under anoxic/reducing conditions.

at grain boundaries. The cumulative time dependent IRF of $^{90}Sr$ under oxic and anoxic/reducing conditions in the time frame of 276 d can be divided in three different regions (Figure 2). The first regions (0 to 5 d) correspond to the highest release rates at the beginning of the experiment, indicating the leaching of the grain boundaries which have an open access to the groundwater and including the contribution of fines leaching (fines located at the periphery of the fuel kernels). Under oxic conditions, the first IRF contribution reached approximately 0.018% within this time period (5 d) while under anoxic/reducing conditions the IRF contribution of 0.13% was determined. Unexpected, the lower release occurred at (air) conditions and might be due to the formation of a protective layer, which lead to a passivation of the grain boundaries. This however needs to be clarified in future with intensive Raman investigations. The second regions (5 to ~ 130 d (air) respectively 5 to 165 d ($Ar/H_2$)) reveal lower release rates. It is assumed that the water needs to diffuse towards grain boundaries which have no direct open access. The third regions (130–276 d (air) respectively 165 to 276 d ($Ar/H_2$) indicate a strong increase in release at (air) conditions. New accessible leaching sites might explain this observation.

Cumulative IRF of $^{137}Cs$ (Figure 3) and $^{134}Cs$ (Figure 3) *vs.* time under (air) and ($Ar/H_2$) in the time frame of investigations (276 d) are comparable. Under oxic environmental conditions of leaching within the first five days, contributions to the IRF were determined to be around 4.8% for $^{134/137}Cs$, indicating leaching of fines and of grain boundaries, which have an open access to the groundwater. No significant further contributions were observed in the next 90 d of leaching. Subsequent, a second relevant release step occurred. Contributions to IRF of 2% for $^{134/137}Cs$ were obtained. After ~ 150 d the release was com-

Bereitgestellt von | Forschungszentrum Juelich
Angemeldet
Heruntergeladen am | 26.06.15 16:04

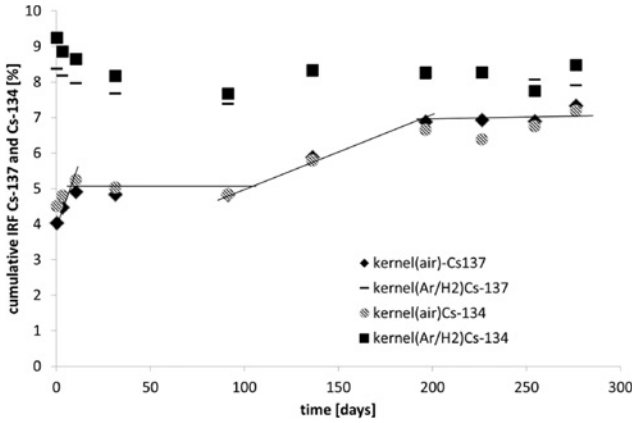


**Fig. 3:** Cumulative IRF of $^{134/137}Cs$ *vs*. time under oxic and under anoxic/reducing conditions.

pleted. As mentioned before, the formation of new accessible leaching sites might explain these observations.

Within the first five days of leaching in ($Ar/H_2$) the highest contributions (around 8% for $^{134/137}Cs$) were obtained. Taken all values into account no further contributions were obtained within the leach period of 276 d. In conclusion, these values of the IRF reflected the Cs fraction located at grain boundaries. Compared to $UO_2$ LWR fuel (60 GWd/t) these values are one order of magnitude higher [13]. As already mentioned, the oxygen potential in LWR fuel is much higher and a large part of Cs is trapped in separated phases (stable ternary Cs compounds ($CsUO_4$, $Cs_2MoO_4$)).

## 3.4 Microstructure evolution

ESEM/EDX technique was used to study the microstructure of the fuel samples. After irradiation the three tight coatings (oPyC, SiC and iPyC) are intact (Figure 4a). Within the buffer region, the formation of a gap occurred indicating the inside pressure build up due to *i.e.* fission gas production. 1.7% of the cross-section surface (grinded to 350 µm in diameter) of the $UO_2$ surface are pores (Figure 4b), the largest having diameters of 20 µm (white circles). Numerous metallic phases (two are marked with white arrows) are visible and contain mainly Mo. In LWR fuel Mo has a buffering effect on the oxygen potential (metallic Mo present in metallic particles is partially oxidised to $MoO_2$) and it is present as $Cs_2MoO_4$ [14]. In the buffer area (white square) besides C (85.32 wt. %) and O (4.86 wt. %) the elements Cs (3.56 wt. %) and Xe (2.52 wt. %) were identified. These findings clearly indicate the high accumulation of Cs and Xe within the buffer and hence their high release from the fuel kernel. After cracking of the coatings the isolated $UO_2$ fuel kernels (Figure 5) were studied by ESEM. The diameter of the fuel kernel increased from 500 µm (before irradiation) to 530 µm. This expansion in diameter is due to enormous production of fission products. At the periphery of the fuel kernel big grains and few intragranular pores (size around 2 µm) are visible (Figure 6a). The grain growth (grain size around 10 µm before irradiation to around 25 µm after irradiation) can be attributed to the coalescence of intergranular pores (located at grain boundaries) [8]. At the periphery numerous hexagonal platelets (Figure 6b) were identified

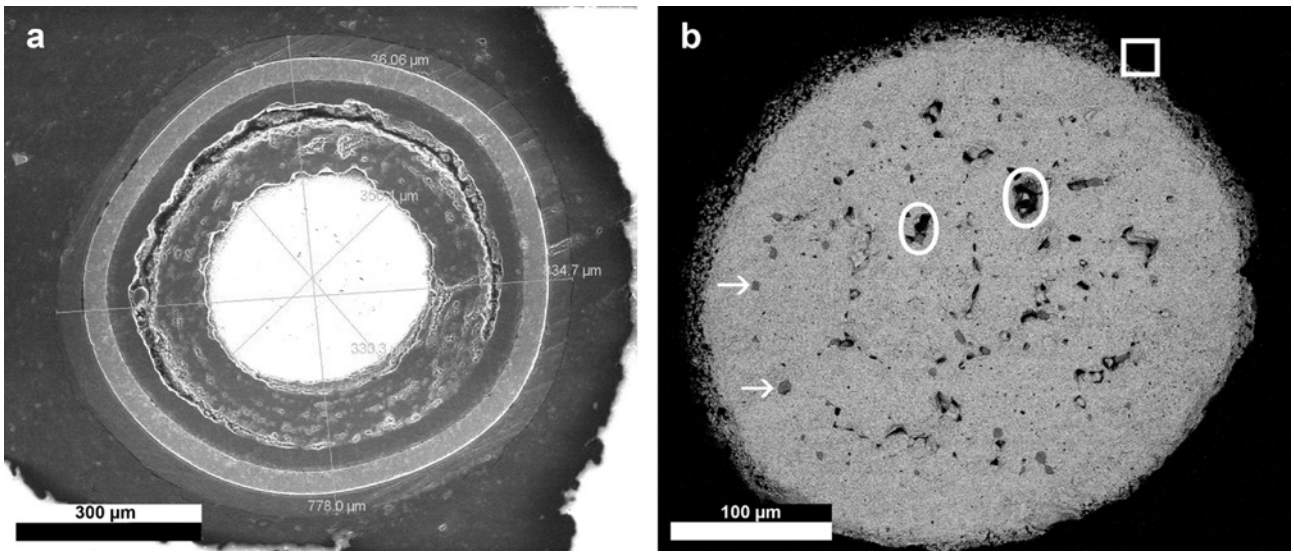


**Fig. 4:** (**a**) Polished TRISO coated fuel particle and (**b**) corresponding cross-section surface of the fuel kernel (white arrow: metallic precipitates; white circles: big pores; white square: buffer area).

Bereitgestellt von | Forschungszentrum Juelich
Angemeldet
Heruntergeladen am | 26.06.15 16:04

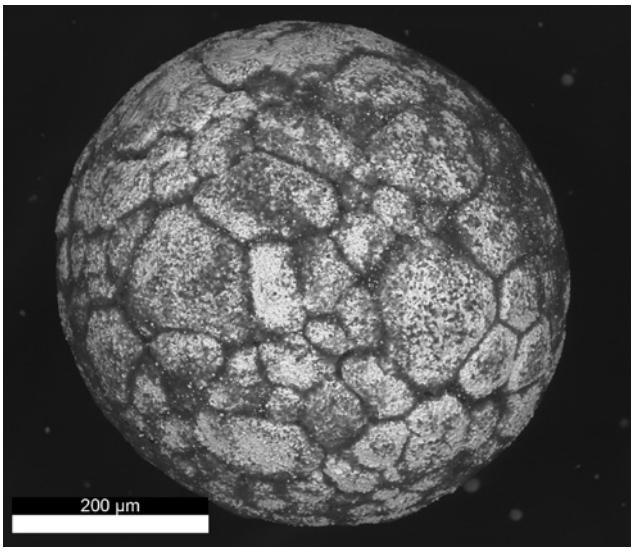


**Fig. 5:** Irradiated $UO_2$ fuel kernel.

and the elements Mo (71.15 wt. %), Tc (17.93 wt. %) and Zr (10.91 wt. %) were detected. The high amounts of Mo within these metallic precipitates confirm the low oxygen potential of this fuel.

Also white spherical spots, containing Mo (42.99 wt. %), Zr (42.57 wt. %) and Tc (14.43 wt. %) are visible.

The influence of leaching on the microstructure is clearly visible. Independently of redox conditions, first, leaching seemed to clean up the surface and the grain boundaries (Figure 6c, d, e and f). This mainly can be attributed to the removal of graphite fines steaming from the carbon buffer after the crack process. Under oxic conditions (Figure 6c and d), white spherical spots containing the elements Mo (52.02 wt. %) and Zr (47.98 wt. %) are visible, but the hexagonal platelets seem to be dissolved and Tc could not be detected (Apollo X Drift detector: detection limit: 0.1 wt. %). Instead, numerous open pores were formed accounting for new assessable leaching sites. Under anoxic/reducing conditions (Figure 6e and f) the pores are filled with platelets hosting the metallic phases (Mo (59.17 wt. %), Ru (21.57 wt. %) and Tc (18.96 wt. %)) and white spots containing Mo (22.51 wt. %) and Zr (77.49 wt. %) were detected. The unexpected association of Zr within the metallic precipitates will be investigated in future in detail. However, this observation underlines the former findings [8], that the expected perovskite phases are not that significant for this fuel type under this irradiation conditions. In general, the metallic particles influence the oxidative matrix dissolution by hydrogen activation and the observed instability of metallic particles in dependency of environmental leaching conditions must be studied in more detail in future.

# 4 Conclusions

To provide knowledge of the fast/instantly released radionuclides from high burn-up spent $UO_2$ fuel, spent TRISO coated particles were used as extremely high burn-up (10.2% FIMA) samples. Each coated particle containing an $UO_2$ fuel kernel which is coated by three tight layers and by a low density carbon layer (buffer), can be described as a miniature fuel element. Due to the tight coatings, no fission gas is released outside during the irradiation process, hence the complete activation/fission products are located in the TRISO coated particles.

By cracking of the coatings an instant gas fraction released. $^{14}C$ as $^{14}CO_2$ and $^{85}Kr$ (up to 35% of the inventory) were identified as gas components. Xe was not detected in the gas fraction but an accumulation within the buffer/iPyC layer was confirmed by ESEM investigations. The observed high fission gas release from the $UO_2$ matrix is different to $UO_2$ LWR spent fuel. The used TRISO particles were irradiated under conditions which enabled re-solution of fission gas from bubbles and like the amount of fission gas present in atomic form within the fuel matrix to diffuse (high thermal diffusivity) to grain boundaries, where it is released. Under the irradiation conditions a low oxygen potential is created by carbon oxidation (CO and $CO_2$ formation) and explain the presence of $^{14}CO_2$.

In a time frame of 276 d leaching experiments have been performed in order to determine the instant radionuclide release fractions under different geochemical environments. U was not detected in solution, indicating insignificant matrix dissolution effects. The contribution of $^{90}Sr$ to the IRF (represents the inventory of $^{90}Sr$ located at grain boundaries) was max 0.2% and comparable to LWR fuel. The behaviour of Cs was found to be very different to LWR fuel. After irradiation 95% of Cs is located within the coatings. Under the as mentioned low oxygen potential of the fuel, ternary Cs compounds are instable. It is assumed that Cs in atomic form released similar to Xe. Within the first five days of leaching under anoxic/reducing conditions, the maximum contribution to the IRF of $^{134/137}Cs$ (8%) was reached, representing the Cs inventory located at the grain boundaries. Compared to LWR spent fuel (60 GWd/t) these values are one order of magnitude higher.

Strongly, the release behaviour of Cs and Sr depend on environmental conditions. Only in oxic environment sec-

Bereitgestellt von | Forschungszentrum Juelich
Angemeldet
Heruntergeladen am | 26.06.15 16:04

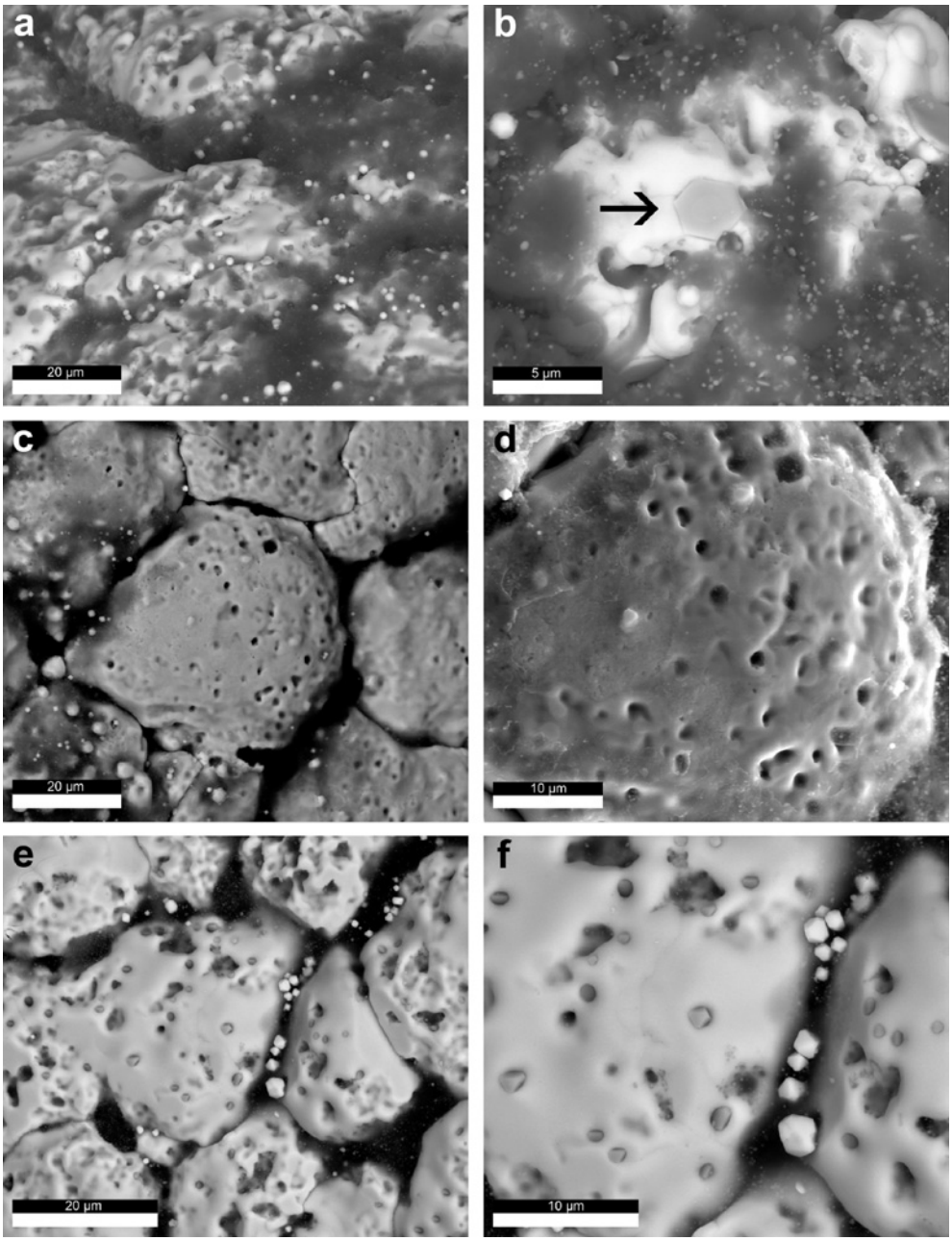


**Fig. 6:** (**a**) Periphery of the irradiated $UO_2$ fuel kernel before leaching, (**b**) hexagonal platelets (arrow) and white spots, (**c**) and (**d**) periphery of the irradiated $UO_2$ fuel kernel after leaching under oxic conditions with grain boundaries, white spots and numerous open intragranular pores, (**e**) and (**f**) periphery of the irradiated $UO_2$ fuel kernel after leaching under anoxic/reducing conditions with grain boundaries, white spots and numerous intragranular pores filled with metallic precipitates.

ond relevant release steps occurred after ~ 100 d, indicating the formation of new accessible leaching sites.

ESEM investigations revealed the influence of leaching on the microstructure. In oxic environment, Tc could not be detected anymore within the white spots (containing Mo and Zr), but the formation of numerous intragranular open pores was observed. Open pores represent new accessible sites for solution attack and might explain the second relevant release steps observed for Cs and Sr. Under anoxic/reducing conditions white spherical spots (containing Mo and Zr) and numerous metallic precipitates (Mo, Tc and Ru) filling the intragranular pores were detected. It can be stated, that leaching in different geochemical environments influenced the speciation of radionuclides which affects the evolution of the microstructure and this directly had an impact on the IRF of radionu-

Bereitgestellt von | Forschungszentrum Juelich
Angemeldet
Heruntergeladen am | 26.06.15 16:04

clides. However, the observed high dissolution rate of Tc under oxic conditions and the association of Zr within the metallic phases are not completely understood and these topics will be investigated in future.

**Acknowledgement:** Special thanks to Sander de Groot and Ralph Hania from Nuclear Research and Consultancy Group in Petten for the TRISO Coated Particles and for their kind support. The research leading to these results has received funding from the European Union's European Atomic Energy Community's (Euratom) Seventh Framework Programme FP7/2007-2011 under grant agreement no. 295722 (FIRST-Nuclides project).

## References

1. Kienzler, B., Altmaier, M., Bube, C., Metz, V.: Radionuclide source term for irradiated fuel from prototype, research and education reactors, for waste forms with negligible heat generation and for uranium tails. KIT Scientific Reports 7365 (2013).
2. Johnson, L. H., Shoesmith, D. H.: *Radioactive Waste Forms for the Future*. (Lutze and Ewing, eds.) Elsevier Science Publishers, B. V. (1988), p. 635.
3. Johnson, L., Günther-Leopold, I., Kobler Waldis, J., Linder, H. P., Low, J., Cui, D., Ekeroth, E.: Rapid aqueous release of fission products from high burn-up LWR fuel: Experimental reults and correlations with fission gas release. J. Nucl. Mater. **420**, 54–62 (2012).
4. Johnson, L. H., Tait, J. C.:Relase of segregated nuclides from spent fuel, SKB technical report 97-18 (1997).
5. Rainer, H., Fachinger, J.: Studies on the long-term behaviour of HTR fuel elements in highly concentrated repository-relevant brines. Radiochim. Acta **80**, 139–145 (1998).
6. Fachinger, J., Exter, M.den., Grambow, B., Holgersson, S., Landessman, C., Titov, M., Produhzina, T.: Nucl. Engin. Design **236**, 543–554 (2006).
7. Fütterer, M. A., Berg, G., Marmier, A., Toscano, E., Freis, D., Bakker, K., de Groot, S.: Results of AVR fuel pebble irradiation at increased temperature and burn-up in the HFR Petten. Nucl. Engin. Design **238**, 2877–2885 (2008).
8. Barrachin, M., Dubourg, R., Groot, S. de, Kissane, M. P., Bakker, K.: Fission-product behaviour in irradiated TRISO-coated particles: Results of the HFR-EU-1bis experiment and their interpretation. J. Nucl. Mater. **415**, 104–116 (2011).
9. Walker, C. T., Rondinella, V. V., Papaioannou, D., Winckel, S. van, Goll, W., Manzel, R.: On the oxidation state of $UO_2$ nuclear fuel at a burn-up of around $100\ \mathrm{MWd/kg}$ HM. J. Nucl. Mater. **345**, 192–205 (2005).
10. Minato, K., Ogawa, T., Fukuda, K., Shimizu, M., Tayamy, Y., Takahashi, I.: J. Nucl. Mater. **20**, 266–281 (1994).
11. Barrachin, M., Dubourg, R., Kissane, M. P., Ozrin, V.: Progress in understanding fission-product behaviour in coated uranium-dioxide fuel particles. J. Nucl. Mater. **385**, 372–386 (2009).
12. Johnson, L. H., Mc Ginnes, D. F.: Partitioning of Radionuclides in Swiss Power Reactor Fuels. NAGRA Technical Report 02-07 (2002).
13. Roudil, D., Jégou, C., Broudic, V., Muzeau, B., Peuget, S., Deschanels, X.: J. Nucl. Mater. **362**, 411–415 (2007).
14. Moriyama, K., Furuya, H.: Thermochemical Prediction of chemical form distribution of fission products in LWR oxide fuels irradiated to high burnup. J. Nucl. Sci. Technol. **34**, 900–908 (1997).

Bereitgestellt von | Forschungszentrum Juelich
Angemeldet
Heruntergeladen am | 26.06.15 16:04